Commun. Comput. Chem. doi: 10.4208/cicc.2016.v4.n3.2

## REGULAR ARTICLE

# The Dynamics of the Reaction of LiH ( $X^1\Sigma^+$ ) with H( $^2S$ ) on a New Potential Energy Surface

Zhen Wang, Meishan Wang\*, Xiaoguang Ma, Chuanlu Yang, Pengfei Wang

School of Physics and Optoelectronics Engineering, Ludong University, Yantai 264025, China Received 25 Nov 2016; Accepted (in revised version) 21 Dec 2016

**Abstract**: The dynamics of the reaction H + LiH are studied with the aid of Quasi-classical trajectory (QCT) method, based on a new ground electronic state global potential energy surface(PES) of Yuan et al.[ Phys. Chem. Chem. Phys. 2015, 17(17):11732-11739]. The influence of collision energy on the dynamic properties of the title reaction is discussed from 0.01eV to 0.8eV. The results show that the variation trend of the dynamics of the H + LiH reaction at low collision energy is markedly different from that of high collision energy. The rotational angular momentum j' of product H<sub>2</sub> is oriented along the positive y-axis all the time. The distributions of PDDCS are calculated and find that the polarized degree of the rotational angular momentum j' is stronger in the forward hemisphere.

AMS subject classifications: 81U10, 81V45, 81V55, 82C05

**Keywords:** Stereodynamics; QCT method; Rotation excitation; Rotational alignment; Reaction mechanism.

#### 1. Introduction

Considerable attention has been paid to the lithium chemistry because of its importance in the evolution of the primordial universe [1-4]. Particularly the LiH formation (via the process of radiative association) and LiH depletion (via the collision with hydrogen atom to form H<sub>2</sub>), which leave the important imprint on the spectrum of the cosmic background radiation from early epochs, are frequently reported during the past decades [5-7]. For the LiH formation, the nascent

<sup>\*</sup> Corresponding author *E-mail address*: mswang1971@163.com (M. - S. Wang). http://www.global-sci.org/cicc

rotational population distribution of LiH (v=0) in the Li (2  $^2P_I$ ) with H $_2$  reaction was studied by Chen et al. [8] using a pump-probe technique in 2000. The results suggested that the reaction be dominated by the insertion mechanism. Bililign et al. [9] observed the LiH formation in the Li\*+H collisions for the atomic states from Li ( $^2$ s) to Li ( $^3$ d). Moreover, the LiH $_2$  system shows the complex features of the more complicated chemical species. Therefore, a series of studies have been carried out about this attractive system recently.

It is well known that the construction of the accurate PES for a reaction system is fundamental to investigate its dynamic properties. So great efforts have been made to construct the PES [10, 11, 18-21, 27, 30, 36] and investigate dynamical properties [10, 12-17, 22-36] for LiH₂ system in the last few decades. Clarke et al. [10] firstly calculated the collinear arrangement PES (CA PES) of the ground-state of LiH2 system, and carried out classical trajectory calculations and time-dependent wave packet propagation studies. Their results showed that the LiH depletion reaction was exothermic with nearly 2.0 eV and existed a small barrier of 0.036 eV in the LiH + H entrance. Dunne et al. [11] constructed an ab initio global PES (DMJ PES) of the lowest state (2A') of LiH2 system using the many body expansion method and the root mean square error (RMSE) of the fitting result was 0.09 eV. It should be noted that the barrier that existed in the LiH + H entrance channel on CA PES couldn't be found in DMJ PES. Based on DMJ PES, a series of quantum mechanical (QM) calculation had been carried out to investigate the dynamics of this reaction in detail [12-17]. Bodo et al. studied the interaction between LiH and H in low energy collision regimes with the Coupled Cluster method when the strength of the coupling between the impinging atom and the ro-vibrational states of LiH was taken into account [18]. Kim et al. [19] constructed an interpolations of accurate ab initio PES and did trajectory calculation to investigate dynamics properties of the LiH formation and depletion reaction. Berriche and Tlili [20] developed an ab initio PES of LiH2 system, in which they observed the presence of a double well for the angles around 11°. Wernli et al. [21] developed a global three-dimensional PES (Wernli PES), which was fitted by large scale calculated energy data in the modified Aguado-Paniagua function and the RMSE was 0.022 eV. Based on the Wernli PES, Bovino et al. [22-26] calculated total reaction probabilities, rate coefficients, and channel reactivity of the reaction LiH + H  $\rightarrow$  Li + H<sub>2</sub> using a time-independent quantum mechanical close-coupling (TIQM-CC) or Time Dependent Wave Packet(TDWP) method. Prudente et al. [27] developed an analytical PES (Prudente PES) and the RMSE was 0.064 eV. Besides, they calculated the reaction probabilities for both exothermic (Li + H<sub>2</sub>) and thermal-neutral (H + LiH) reaction by using real wave packet (RWP) method. Based on the Prudente PES, Jiang et al. [28-34] investigated the dynamics of the reaction H + LiH using QCT or QM method. Hsiao et al. [35] constructed ab initio PES of the ground 12A' and excited 22A' states of LiH2 system. Recently, Yuan et al. [36] employed neural network method to construct a new ground electronic state global PES (YHC PES) of LiH2 system. The accuracy of fitting procedure of the YHC PES is fairly high with only 0.004eV. The spectroscopic constants of LiH  $(X^1\Sigma^+)$  and  $H_2(X^1\Sigma_g^+)$  obtained from the YHC PES agreed very well with the experimental data.

Subsequently the simple scalar properties of the reaction H ( $^2$ S) + LiH ( $X^1\Sigma^+$ )  $\rightarrow$  Li ( $^2$ S) + H<sub>2</sub> ( $X^1\Sigma^+$ ) were studied with TDWP method.

Comparing with Prudente PES and Wernli PES, the YHC PES seems to be more accurate and the spectroscopic constants obtained from it agreed very well with the experimental data. So in order to an accurate understanding of the H+LiH reaction, we calculate its dynamics based on the YHC PES. In this paper, we study the effect of collision energy on the dynamics of the title reaction in detail. This paper is organized as follows: in Section 2, the basic theory is given. In Section 3, the results and discussion are presented. Finally, Section 4 closes with the conclusion.

## 2. Theory

The QCT method is well established to deal with the bimolecular reactive collision processes and has been very successfully applied to numerous atom-diatom and diatom-diatom chemical reactions in recent years. Since the details of such methods are well documented in the literature [37-42], we will be concerned only with the essentials here.

In this calculation, the initial conditions are selected by a standard Monte Carlo sampling and the adaptive-step Adams and Runge-Kutta method are employed to ensure the adequacy and the stability of the trajectory integrator. The vibrational and rotational levels of the reactant molecule are taken as v=0, j = 0 respectively. Batches of 100 000 trajectories are calculated as the sample for each condition. The integration step is chosen to be 0.1 fs and the initial distance between H atom and the center of the mass of LiH molecule is 15 Å for every trajectory. Reaction probabilities and integral cross section, as a function of collision energy ( $E_t$ ) for the H + LiH reaction, have been calculated at the randomly and uniformly sampled collision energies within the range 0.01~0.8 eV. The total reaction probability as the impact parameter b = 0, can be written by:

$$P(E_{t}, v, j) = \lim \frac{N_{r}(E_{t}, v, j)}{N_{t}(E_{t}, v, j)}$$
 (1)

The reaction cross section  $\sigma_{\nu}(E_{\nu}, \nu, j)$  can be written as:

$$\sigma_r(E_t, \mathbf{v}, \mathbf{j}) = \pi b_{\text{max}}^2 \lim \frac{N_r(E_t, \mathbf{v}, \mathbf{j})}{N_r(E_t, \mathbf{v}, \mathbf{j})}$$
(2)

The  $b_{max}$  is the maximum impact parameter for the different collision energy and listed in **Table 1**.

Collision energy(eV)	0.01	0.05	0.1	0.2	0.3	0.4	0.5	0.6	0.7	0.8
b <sub>max</sub> (Å)	5.985	4.800	4.303	3.760	3.625	3.570	3.530	3.490	3.460	3.420

Table 1. Maximum impact parameters.

The impact parameter used, ensure that no reaction occurs at a given collision energy for values of the impact parameter larger than  $b_{max}$ . For the equation that describes the rotational polarization of the product, they are listed in the appendix.

## 3. Results and discussion

# 3.1 Topological features of the YHC PES

Yuan et al. analyzed the topographical features and minimum energy paths of the YHC PES at four different Li–H–H angles (180°, 135°, 90°, and 45°) [36].

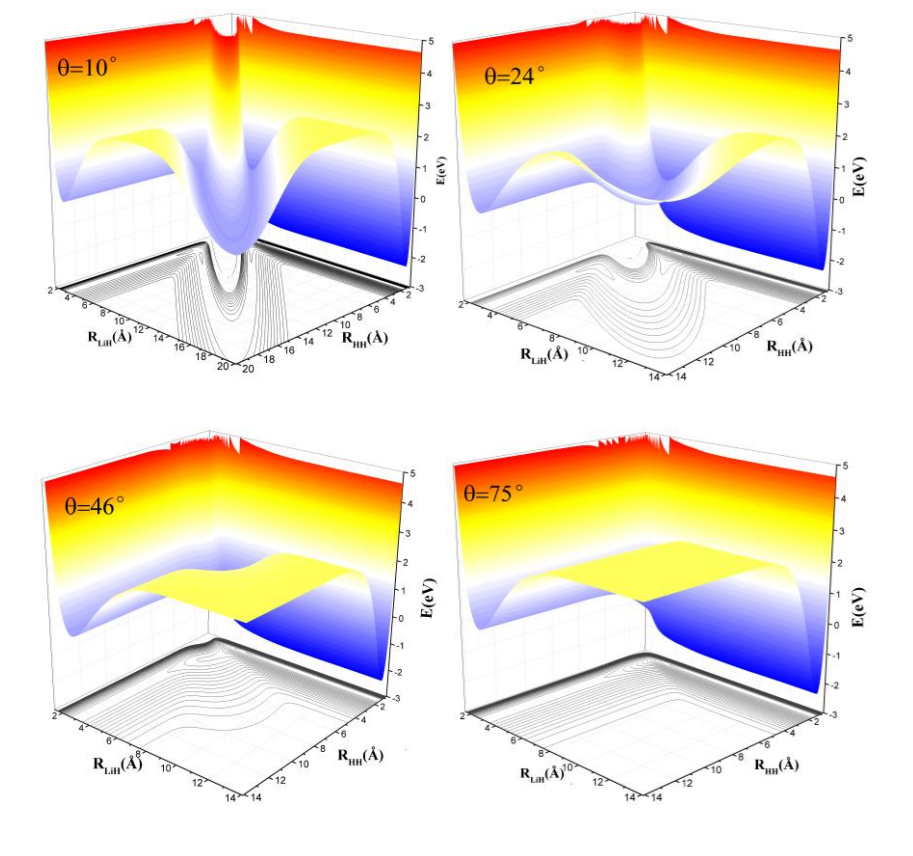


**Figure 1**: Potential energy surfaces for the four Li-H-H angles 10°, 24°, 46°, 75°.

Two valleys are found in each of the four angles: the product valley of Li+ H₂ is deeper than the reactant valley of H + LiH because of the exothermicity of H + LiH → Li + H₂. But, they have not analyzed the topographical features and minimum energy paths of the YHC PES at the small Li–H–H angle, which play an important role in the dynamic calculation. In order to compare with the other PES, we further analyze the topographical features and minimum energy paths, which are shown in **Figures 1** and **2**, respectively. **Figure 1** provided the topographical features of the YHC PES at four different Li–H–H angles (10°, 24°, 46°, and 75°). One can find from Figure 1a that there is double well to exist in the entrance side of the PES when Li–H–H angle is less than 24°, which is in accord with the PES constructed by Berriche and Tlili [20]. The energy barrier between the double well will weaken with the increase of Li–H–H angle. As the Li–H–H angle reaches 24° (**Figure 1b**), the double well will turn into a single deeper well until Li–H–H angle approach to 46°. When the angle of approach to 46° (**Figure 1c**), the well disappear entirely.

The minimum energy paths (MEPs) from LiH to  $H_2$  at four different Li–H–H angles given in **Figure 2** clearly show that there is double well or single well when the Li–H–H angles is less than  $46^{\circ}$ .

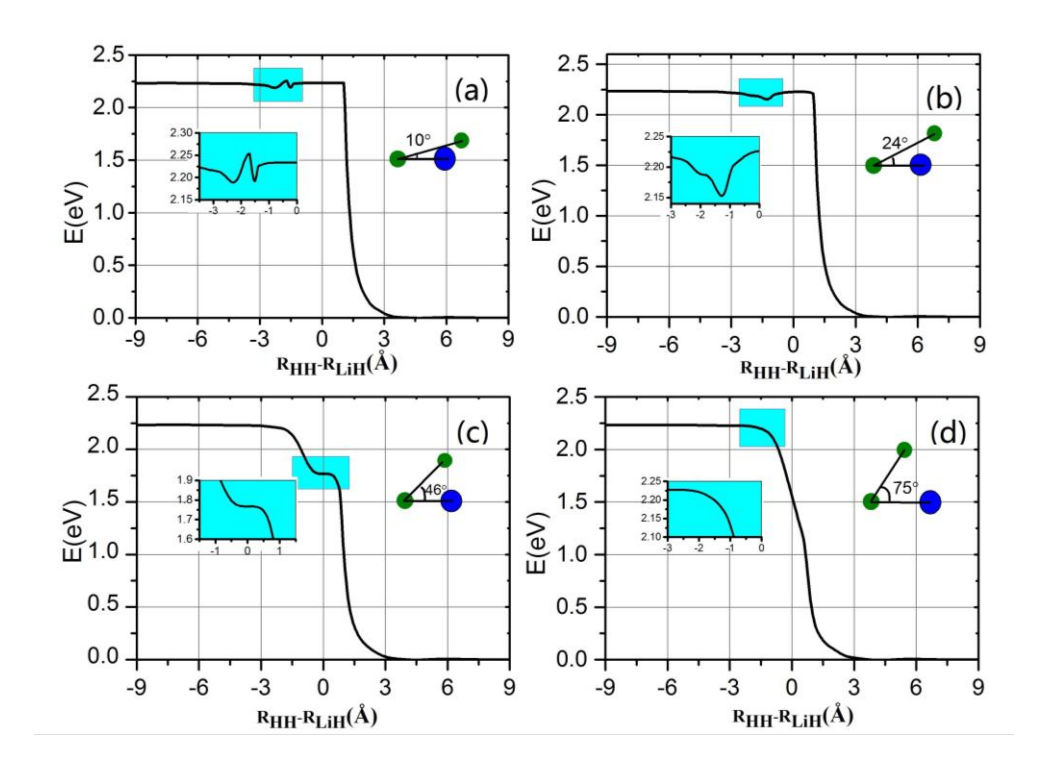
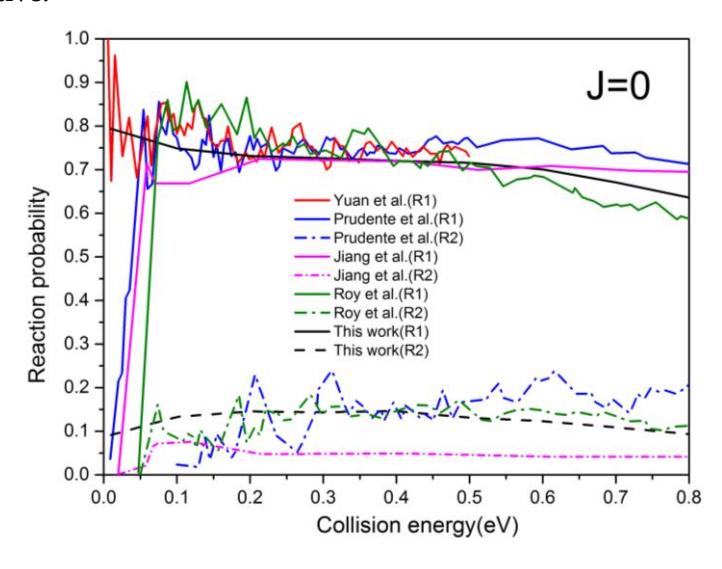


Figure 2: Minimum energy paths for the LiH<sub>2</sub> PES at four Li-H-H angles

# 3.2 Reaction probability and integral cross section

The reaction probability of the LiH depletion (R1) and H-exchange (R2) channels with J = 0 are calculated by running batches of 100000 trajectories with a zero impact parameter (b=0) as a function of collision energy. The obtained results and previous results are shown in **Figure 3**.

In order to certify the validity of our calculations, we firstly compare the QCT probabilities with the quantum results, which have been calculated by TDWP method on the YHC PES [36]. It is obvious from **Figure 3** that the QCT results are in general agreement with the quantum results. However, there is still a tiny difference. The QCT calculations can't reproduce the strong resonance structures character that can emerge on the curve of the TDWP reaction probabilities. Subsequently, we compare our results with the QCT results of Jiang et al. [31] that are calculated on Prudente PES [27]. The results are mainly the same except for the collision energy less than 0.2eV. The reason is that there is an early energy barrier on the Prudente PES, which cannot be found in YHC PES. All of the results show that the reaction probability of the LiH depletion is higher than H-exchange channel. Generally speaking, a free atom A prefers to react with the low electronegative atom of BC molecule in the reaction process of A+BC [43]. Therefore, the free atom H has priority to attack the H of LiH to form H<sub>2</sub> in the reaction H + LiH, because the electronegativity of H is weaker than Li. In addition, the reaction probabilities are very high at low collision energies, which imply that the PES is attractive.



**Figure 3**: Comparison of the reaction probabilities between the QCT (our results and cf.Fig.1 of Ref. 31) and QM (cf. Fig. 1 of Ref. 24 and Fig. 3 of Ref. 27) calcula -tions of LiH depletion (R1) and H exchange (R2) channels.

The integral cross section (ICS) values for the reaction H + LiH at v=0, j=0 state in the collision energy range 0.01~0.8ev are calculated and compare with the quantum results [24, 27, 36] based on Wernli PES, Prudente PES and YHC PES in **Figure 4**.

One can find that the ICS depends strongly on collision energy and decrease monotonically with the increase of collision energy. It can be explained by the topographical character of the YHC PES. The YHC PES is a typical attractive potential energy surface. And for this PES, the reaction is principally dominated by the centrifugal potential that has a direct relationship with collision energy. The centrifugal potential increase with the increase of collision energy, which results in the reducing of the ICS values. Our QCT results are in agreement with the quantum results of Yuan et al.

#### 3.3 The reaction mechanism

To clarify the reaction mechanism, the variations of internuclear distances of H<sub>a</sub>-H<sub>b</sub>, Li-H<sub>a</sub>, and Li-H<sub>b</sub>, as functions of propagation time by random selecting reactive trajectory of different collision energy, are presented in **Figure 5**.

As can be seen in **Figure 5(a)**, the strange phenomenon is found that the internuclear distances of H<sub>a</sub>-H<sub>b</sub>, Li-H<sub>b</sub> increase suddenly before the collision occurs. It is caused by the reason of the repulsive wall provided by Li atom. From the **Figure 5(b)**, one can find that the attacking atom H collides with the target molecule LiH to form the short lifetime (about 10<sup>-13</sup>s) complexes LiHH before breaking-up into the LiH depletion channel.

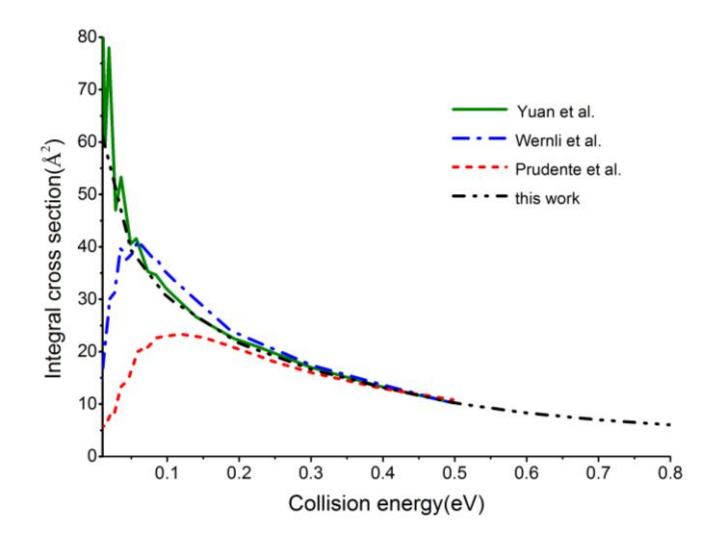


**Figure 4**: Comparison of total integer cross section between the present results and previous theoretical results that calculated on the YHC PES [Ref. 36], Prudente PES [Ref. 27] and Wernli PES [Ref. 24] using TDWP method for the LiH depletion reaction.

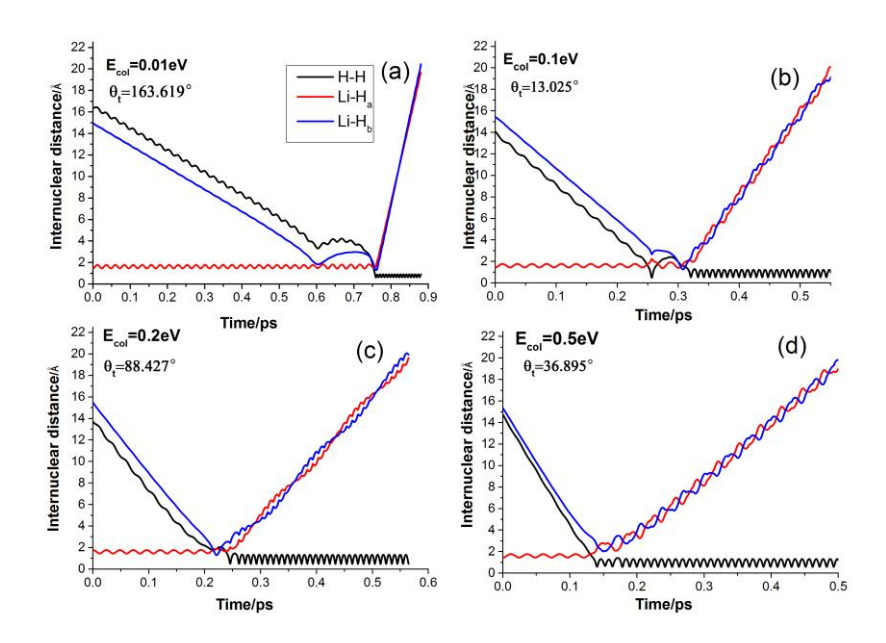


**Figure 5**: Internuclear distances of  $H_a$ - $H_b$ , Li- $H_a$ , and Li- $H_b$  as a function of propagation time, with the fixed scattering angle  $\theta$ . The collision energy is 0.01eV, 0.1 eV, 0.2 eV and 0.5 eV respectively.

In order to verify whether the emergence of complex associated with shallow potential well, the value of potential energy of reaction process as the function of collision time are calculated and plotted in in **Figure 6**.

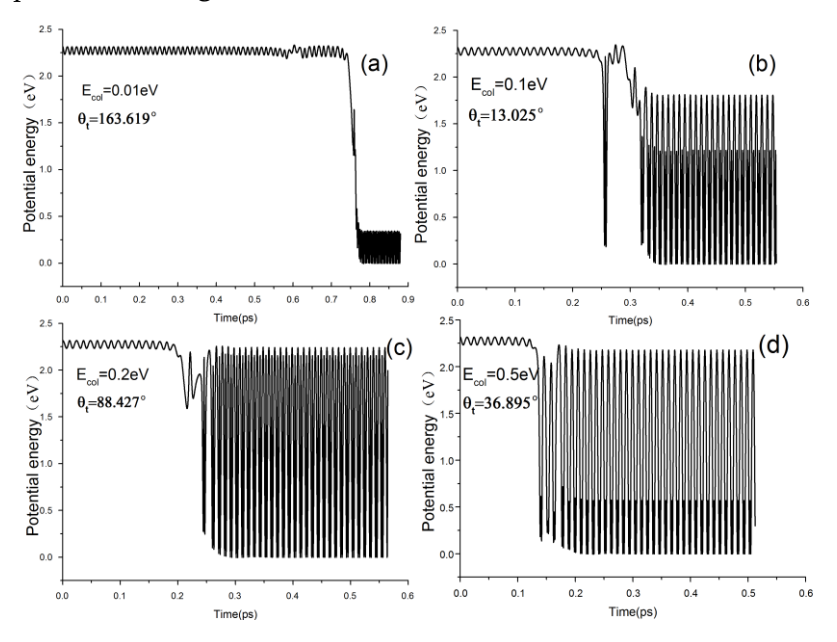


**Figure 6**: Potential energy of  $H_a$ - $H_b$ -Li as a function of propagation time, with the fixed scattering angle  $\theta$ .

As can be seen from **Figure 6(b)**, the potential energies suddenly decrease during the formation of complexes. Combined with the minimum energy paths plotted in **Figure 1(b)**, the existence of complex is confirmed to be connected with the potential well. When the collision energy is higher than 0.2eV, as can be seen in **Figure 5(c)** and **5(d)** respectively, the reaction process is very rapid and the indirect reactive trajectories can't be found. The variation of potential energies can be seen in **Figure 6(c)** and **(d)** respectively. Besides, the oscillation amplitude of the product H<sub>2</sub> become strong with the increase of collision energy, which signify the vibration level of the product H<sub>2</sub> is excited to a higher vibrational state. Overall, the reaction H + LiH is mainly controlled by the direct reaction mechanism. However, the formation of intermediate complex indicates that the indirect mechanism plays a role during the reaction process of low collision energies.

# 3.4 The polarized distributions of the $P(\theta_r)$ , $P(\phi_r)$ , $P(\theta_r, \phi_r)$

The  $P(\theta r)$  distributions of the product H<sub>2</sub> at the selected collision energies (0.01ev, 0.1ev, 0.2ev, 0.5ev, and 0.8eV) are presented in **Figure 7**, which reflects k-j' vector correlation.

As can be seen from **Figure 7**, the  $P(\theta r)$  distribution exits a maximum at the  $\theta \approx 90^{\circ}$  and is symmetrical with respect to  $90^{\circ}$  at the given collision energy, which indicates that the product angular momentum j' is aligned along the direction perpendicular to the initial relative velocity direction k. When the collision energy increases from 0.2 eV to 0.8 eV, the peak of

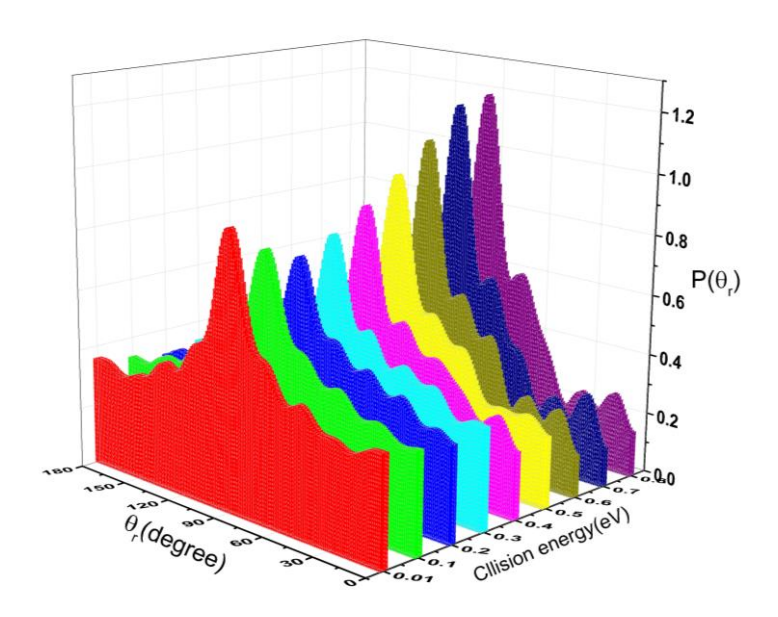


**Figure 7**: The distribution of  $P(\theta)$  as a function of polar angle  $\theta$  at five collision energy (0.01eV, 0.1 eV, 0.2 eV, 0.5 eV and 0.8eV) is plotted.

 $P(\theta)$  distribution becomes higher and broader, which indicates the degree of alignment of H<sub>2</sub> from the reaction H + LiH becomes stronger with the increase of collision energy. It is in well agreement with the previous results [29, 30]. However, when the collision energy increases from 0.01 eV to 0.2 eV, an opposite tendency is showing that the peak of  $P(\theta)$  distribution becomes lower and narrower, which indicates that the rotational alignment degree of the product becomes weaker. This phenomenon can be explained by the reason that the well that exists around H of LiH diatom [36], contribute to the rotational alignment degree of the product H<sub>2</sub> when the collision energy is small. With the increase of collision energy, the effect of well become small, which lead the alignment degree to weaken. When the collision energy is higher, the translational energy of H atom acts as a mainly factor for the distribution of the product rotational alignment. In order to obtain a better understanding of the alignment degree of the product, we calculate the product alignment parameter  $\langle P_2(j' \cdot k)\rangle$ , which are shown in **Figure 8**.

For the product alignment parameter, there exists a classical limiting value of -0.5, the closer the value of the parameter approaches -0.5, the stronger the product is aligned along the direction perpendicular to k. It is obviously seen from Figure 8 that the calculated values of  $\langle P_2(j' \cdot k) \rangle$  are agree with the distribution of  $P(\theta_t)$ .

The  $P(\phi_r)$  distributions shown in **Figure 9** describe the k-k'-j' vector correlations at five collision energies  $E_{col} = 0.01$ ev, 0.1ev, 0.2ev, 0.5ev, and 0.8eV, which reveals the rotational polarization of product  $H_2$  and its collision energy-dependent behaviors.

Some similar features for the five collision energies of the title reaction are found: the  $P(\phi_r)$  distributions are asymmetric with respect to the k-k' scattering plane (or about  $\phi_r$ =180°) and there are two peaks appear around  $\phi_r$  = 90° and 270°. The peak at  $\phi_r$  angle closes to 90° indicates a preference for right-handed product rotation while the peak in the  $P(\phi_r)$ 

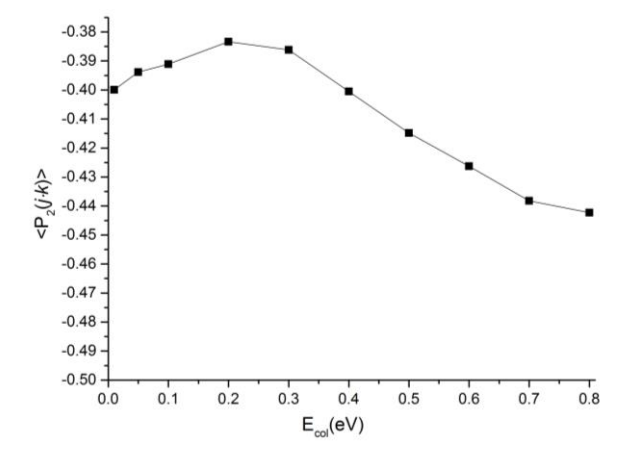


**Figure 8**: The rotational alignment parameters of the product H<sub>2</sub> for the reaction H + LiH (v = 0, j = 0)  $\rightarrow$  H<sub>2</sub> + Li at several collision energies.

distribution at  $\phi$  angle closes to 270° implies a preference for left-handed product rotation. The peaks of  $P(\phi_r)$  appearing at  $\phi_r = 90^\circ$  and 270° indicate that the rotational angular momentum vectors of the products are mainly aligned along the y-axis of the CM frame. One can be found from **Figure 9** that the peak at  $\phi = 90^{\circ}$  is higher than  $\phi = 270^{\circ}$ , which indicates that the rotational angular momentum vectors of the H2 are not only aligned but also oriented along the positive direction of y-axis of the CM frame. When the collision energy increases from 0.01eV to 0.1eV, the two peaks at  $\phi = 90^{\circ}$  and 270° both become lower, which means that the rotational alignment degree of the product along the y-axis of the CM frame dramatically weaken. However, when collision energy increases from 0.2 eV to 0.8eV, the peak at  $\phi$ =90° significantly heightens while the peak at  $\phi$  =270° becomes a little lower, which means that the orientation degree of the product along the positive direction of y-axis of the CM frame evidently strengthen. It should be specially mentioned that the  $P(\phi_r)$  distribution based on the YHC PES has significant difference from the  $P(\phi_r)$  distribution based on the Prudente PES [27] at low collision energy. The rotational angular momentum vectors of the H<sub>2</sub> are oriented along the positive direction of y-axis all the time in this paper; however, they are oriented along the negative direction of y-axis of the CM frame in the results of Jiang et al. [30]. The main reason is that the Prudente PES exists a barrier but not find in YHC PES.

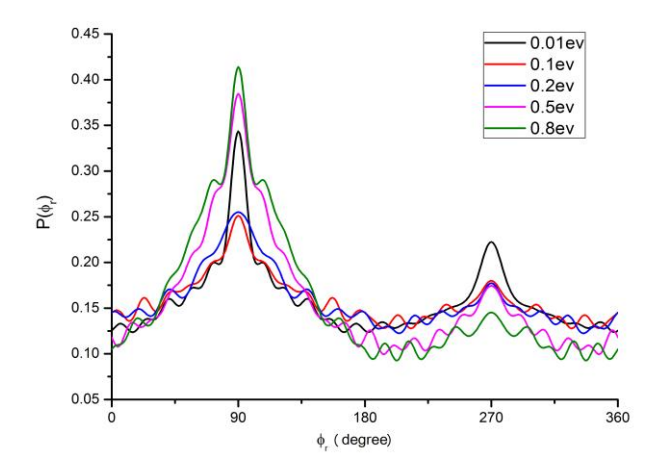


**Figure 9**: The distribution of  $P(\phi_r)$  for the H (2S) + LiH (X<sup>1</sup> $\Sigma$ <sup>+</sup>)  $\rightarrow$  Li (2S) + H<sub>2</sub> (X<sup>1</sup> $\Sigma$ <sub>g</sub><sup>+</sup>) reaction at five collision energy as a function of azimuthal angle  $\phi_r$ 

In order to better understand the rotational polarization of the product H<sub>2</sub>, we calculated the  $P(\theta_r, \phi_r)$  distributions in the form of polar plots in **Figure 10** for a series of collision energy. It is evident that the distributions  $P(\theta_r, \phi_r)$ , which peak at (90°, 90°) and (90°, 270°), are consistent very well with the distributions of  $P(\theta_r)$  and  $P(\phi_r)$ . The distributions  $P(\theta_r, \phi_r)$  also

show that the products H<sub>2</sub> are preferentially polarized perpendicular to the scattering plane and rotate in planes parallel to the scattering plane.

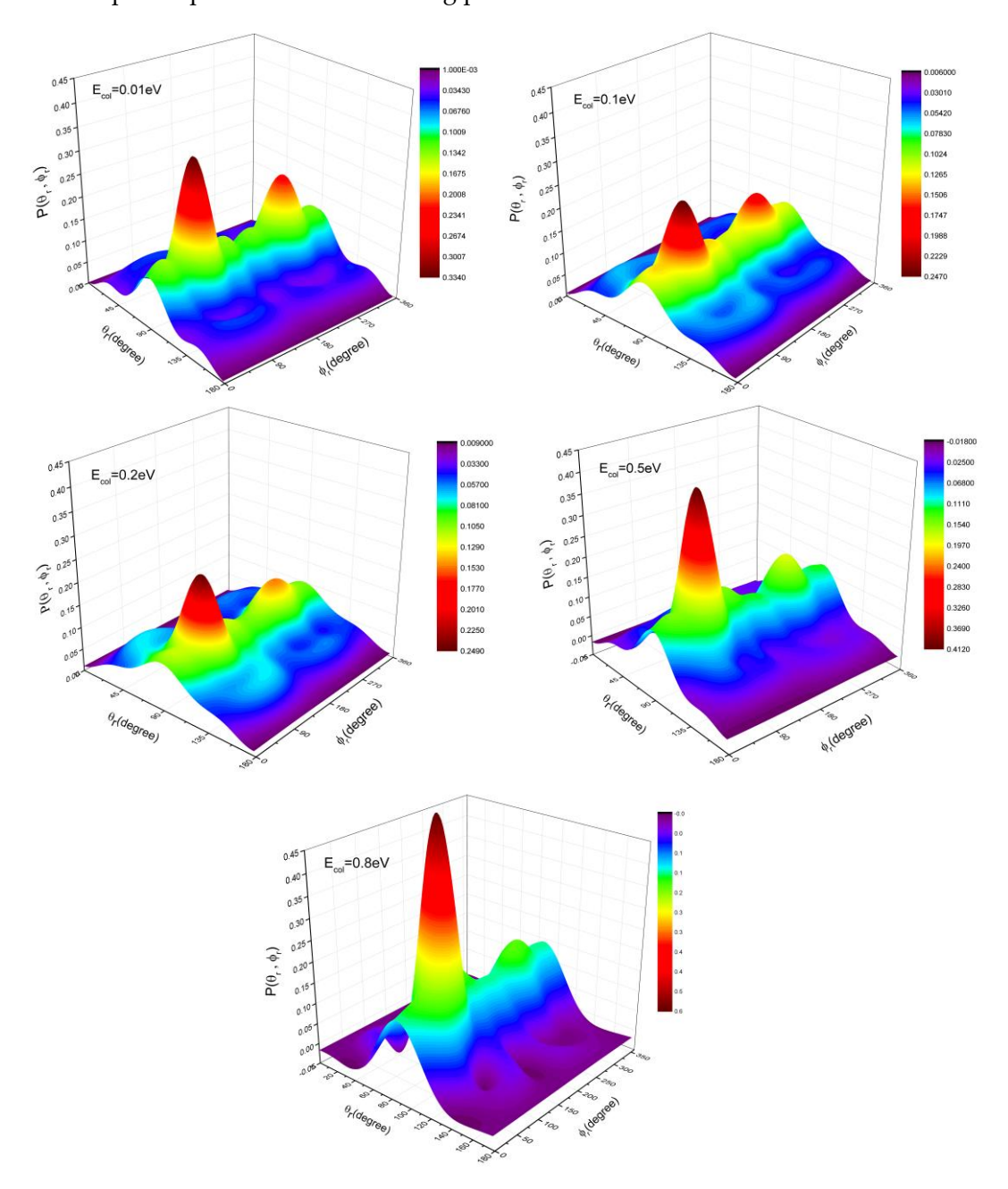


**Figure 10**: The  $P(\theta_r, \phi_r)$  distribution at the five collision energies (0.01ev, 0.1ev, 0.2ev, 0.5ev, 0.8ev) for H + LiH (v = 0, j = 0)  $\rightarrow$  Li+ H<sub>2</sub> reaction.

## 3.5 The distribution of PDDCS

The calculated results of the PDDCS for the five different collision energies are shown in **Figure 11**.

The  $(2\pi/\sigma)(d\sigma_{00}/d\omega_t)$  distribution corresponds to a simple differential cross-section (DCS), which describes the k-k' correlation. The scattering direction of the product molecules is mainly dominated by the forward scattering and the sideway and backward scattering are weakly visible. The tendency of the forward scattering increases remarkably with the increase of the collision energy while the sideway and backward scattering always weakly appear, which can be explained by using the purely impulsive effect [30]. One can be found from **Figure 11(a)** that the results of  $(2\pi/\sigma)(d\sigma\omega/d\omega)$  are well agreement with the results of Jiang et al [30]. As can be seen in Figure 11(b), the negative value becomes much larger as the collision energy increases from 0.2ev~0.8ev, which is in accordance with the results of Jiang et al [30], however, the negative value of  $(2\pi/\sigma)(d\sigma_{20}/d\omega_t)$  at the extreme forward direction ( $\theta_t$ =0°) is decreased when collision energy increases from 0.01~0.2ev. When the scattering angle  $\theta$ <40°, the polarization of j' along the direction perpendicular to k firstly decreases and then increases with the increase of collision energy. This variation tendency is in agreement with the distribution of  $P(\theta)$ . At the extremities of forward ( $\theta=0^{\circ}$ ) and backward ( $\theta=180^{\circ}$ ) scattering, the  $(2\pi/\sigma)(d\sigma_{22+}/d\omega_t)$  and  $(2\pi/\sigma)(d\sigma_{21-}/d\omega_t)$  values equal to zero. **Figure 11(c)** shows the values of  $(2\pi/\sigma)(d\sigma_{22+}/d\omega_t)$  are basically negative for all scattering angles, which indicates the j' of product H<sub>2</sub> prefers to align along the y-axis. With the increasing of collision energy, the negative value of  $(2\pi/\sigma)(d\sigma_{22+}/d\omega_t)$  firstly decreases and then strongly increases, therefore, one can conclude that the degree of the polarization of the product H2 firstly weakens and then enhances with the increasing of collision energy. The products display a stronger polarization at  $\theta$  close to 30°, 90° and 135° at the collision energy of 0.8 eV. The variation trend of  $(2\pi/\sigma)(d\sigma_{22+}/d\omega_t)$  with scattering angle is similar with the results of Jiang et al at the same collision energy [30]. The distribution of  $(2\pi/\sigma)(d\sigma_{21}/d\omega_t)$ , which is related to  $\langle \sin^2\theta\cos^2\phi_t \rangle$ , can be seen in Figure 11(d). At the collision energy of 0.01~0.2eV, that the values of  $(2\pi/\sigma)(d\sigma_{21}/d\omega_t)$  are positive and nearly close to zero. This result indicates that j' is aligned along the direction of vector x+z (in the forward hemisphere) and the polarization of the product H<sub>2</sub> is not evident. But the value of  $(2\pi/\sigma)(d\sigma_{21}/d\omega_t)$  becomes higher in the scattering angle ranges of 0~45° with the increase of the collision energy, which indicates that the polarization of j' of the product H<sub>2</sub> in the forward hemisphere becomes evident as the collision energy increases. One also can find that the strongest polarization of the product H<sub>2</sub> is in 20° from the **Figure 11(d)**. It must be said that the values of  $(2\pi/\sigma)(d\sigma_{21}/d\omega_t)$  are positive (in the scattering angle ranges of 0° to 40°) at all of the selected collision energy, however, the corresponding value of Jiang et al [30] is negative at the low collision energy (<0.4eV), which

is in part because of the barrier existed on the Prudente PES.

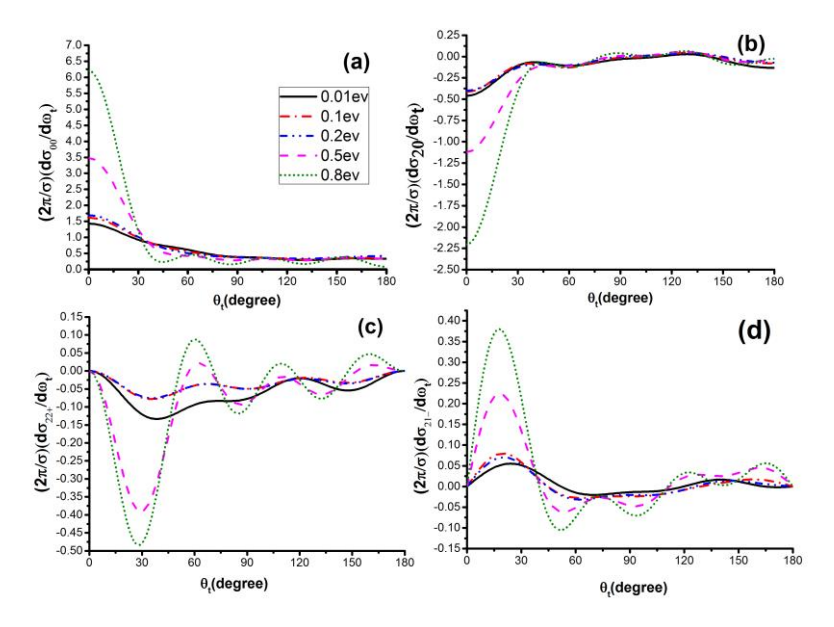


**Figure 11**: Four PDDCSs for the H (2S) + LiH (X1 $\Sigma$ +)  $\rightarrow$  Li (2S) + H2 (X1 $\Sigma$ g+) reaction at five collision energy are plotted as a function of scattering angle  $\theta$ 

## 4. Conclusion

In this paper, we firstly analyze the topological features of the YHC PES in detail, which exists the double-well or single-well as well as the repulsive wall when Li-H-H angle is small. Therefore, the YHC PES presents significant new feature comparing with the previous PES [11, 20, 21, 27]. Based on the YHC PES, we calculate the stereodynamics of the H + LiH reaction at five selected collision energies of 0.01 eV, 0.1 eV, 0.2 eV, 0.5 eV, and 0.8eV. The results show that the variation trend of the dynamics of the title reaction at low collision energy is markedly different from that of high collision energy. The reaction probability and integral cross section both decrease with the increase of collision energy, which indirectly prove the existence of the well. The indirect reaction mechanism plays a role during the reaction process of the reaction H + LiH at low collision energy, although the reaction process is mainly dominated by the direct reaction mechanism at high collision energy. The degree of alignment of the rotational angular momentum j' of product H<sub>2</sub> becomes firstly weaken and then strengthen with the increase of collision energy. Besides, the j' is not only aligned but also always oriented along the positive y-axis. The normalized PDDCSs show that the polarized degree of the rotational angular momentum j' is stronger when scattering angle less than 45°. Comparing with the results of Jiang et al., the variation tendency of  $(2\pi/\sigma)(d\sigma_{00}/d\omega_t)$ ,  $(2\pi/\sigma)(d\sigma_{20}/d\omega_t)$ , and  $(2\pi/\sigma)(d\sigma_{22}t/d\omega_t)$ , are basically similar. However, the

values of  $(2\pi/\sigma)(d\sigma_{21}/d\omega_t)$  are positive in the scattering angle ranges of  $0^\circ$  to  $40^\circ$  at all of the selected collision energy, however, the corresponding value of Jiang et al [30] is negative at the low collision energy (< 0.4eV). These results indicate that j' is aligned along the direction of vector x + z in the forward hemisphere at all the collision energy.

# Acknowledgements

This work was supported by the National Natural Science Foundation of China (Grant No. 11474142), Natural Science Foundation of Shandong Province (Grant Nos. ZR2014AM 0005 and ZR2014AQ022), Taishan Scholarship Project of Shandong Province. All calculation data were carried out in the Tiansuo Super Computer Center (TSCC) of Ludong University. The authors appreciate Professor Han for providing the QCT codes and are also very grateful to Professor Maodu Chen for providing the data of the potential energy surface.

#### References

- [1] S. Lepp, J.M. Shull, Molecules in the early universe, Astrophys J., 280 (1984), 465-469.
- [2] S. Lepp, P.C. Stancil, A. Dalgarno, Atomic and molecular processes in the early Universe, J. Phys. B., 35 (2002), 1-24.
- [3] E. Bodo, F.A. Gianturco, R. Martinazzo, The gas-phase lithium chemistry in the early universe: Elementary processes, interaction forces and quantum dynamics, Phys. Rep., 384 (2003), 85-119.
- [4] N. Yoshida, T. Abel, L. Hernquist, N. Sugiyama, Simulations of Early Structure Formation: Primordial Gas Clouds, Astrophys J., 592 (2003), 645-663.
- [5] V. Dubrovich, A. Lipovka, Distortions of the cosmic blackbody spectrum due to luminescence of H<sub>2</sub>D<sup>+</sup> molecules, Astron. Astrophys., 296 (1995), 301-306.
- [6] P. Stancil, S. Lepp, A. Dalgarno, The lithium chemistry of the early Universe, Astrophys. J, 458 (1996), 401.
- [7] P. Stancil, A. Dalgarno, Stimulated radiative association of Li and H in the Early Universe, Astrophys. J, 479 (1997), 543.
- [8] S. Bililign, B.C. Hattaway, T.L. Robinson, G.-H. Jeung, Far-wing scattering studies on the reaction Li\*(2p, 3p)+  $H_2 \rightarrow LiH$  (v "= 1, 2, J ")+ H, J. Chem. Phys, 114 (2001), 7052-7058.
- [9] J.-J. Chen, Y.-M. Hung, D.-K. Liu, H.-S. Fung, K.-C. Linb, Reaction pathway, energy barrier, and rotational state distribution for Li  $(2^2P_1)$  + $H_2 \rightarrow \text{LiH}(X^1\Sigma^+)$ +H, J. Chem. Phys., 114 (2001), 9395-9401.
- [10] N.J. Clarke, M. Sironi, M. Raimondi, S. Kumar, F.A. Gianturco, E. Buonomo, D.L. Cooper, Classical and quantum dynamics on the collinear potential energy surface for the reaction of Li with H<sub>2</sub>, Chem. Phys., 233 (1998), 9-27.
- [11] L.J. Dunne, J.N. Murrell, P. Jemmer, Analytical potential energy surface and quasi-classical dynamics for the reaction LiH (X,  $^1\Sigma^+$ )+ H ( $^2S$ ) $\rightarrow$  Li ( $^2S$ )+ H2 (X,  $^1\Sigma^+$ g), Chem. Phys. Lett., 336 (2001), 1-6.
- [12] P. Defazio, C. Petrongolo, P. Gamallo, M. González, Product distributions, rate constants, and

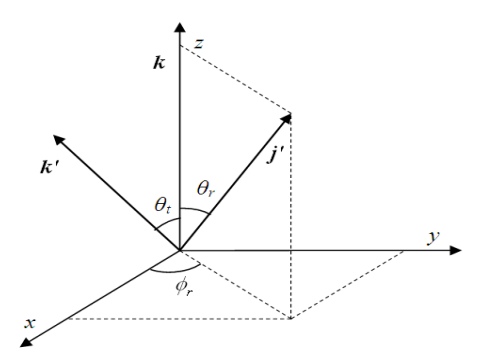
- mechanisms of LiH+ H reactions, J. Chem. Phys, 122 (2005), 214303.
- [13] R. Padmanaban, S. Mahapatra, Time-dependent wave packet dynamics of the H+HLi reactive scattering, J. Chem. Phys, 117 (2002), 6469-6477.
- [14] R. Padmanaban, S. Mahapatra, Resonances in three-dimensional H+HLi scattering: A time-dependent wave packet dynamical study, J. Chem. Phys, 120 (2004), 1746-1755.
- [15] R. Padmanaban, S. Mahapatra, Quantum wave-packet dynamics of H+ HLi scattering: Reaction cross section and thermal rate constant, J. Chem. Phys, 121 (2004), 7681-7691.
- [16] R. Padmanaban, S. Mahapatra, Resonances in H+HLi scattering for nonzero total angular momentum (J> 0): a time-dependent wave packet approach, J. Theor. Comput. Chem., 5 (2006), 871-885.
- [17] R. Padmanaban, S. Mahapatra, Coriolis-coupled wave packet dynamics of H+ HLi reaction, J. Phys. Chem. A, 110 (2006), 6039-6046.
- [18] E. Bodo, F. Gianturco, R. Martinazzo, M. Raimondi, Computed orientational anisotropy and vibrational couplings for the LiH+ H interaction potential, Eur. Phys. J. D., 15 (2001), 321-329.
- [19] K.H. Kim, Y.S. Lee, T. Ishida, G.-H. Jeung, Dynamics calculations for the LiH plus H→ Li+ H₂ reactions using interpolations of accurate ab initio potential energy surfaces, J. Chem. Phys., 119 (2003), 4689-4693.
- [20] H. Berriche, C. Tlili, Ab initio potential energy surface and rotationally inelastic collisions of LiH ( $X^1$   $\Sigma^+$ ) with H.I. The ab initio evaluation of the potential energy surface, J. Mol. Struct. Theochem., 678 (2004), 11-16.
- [21] M. Wernli, D. Caruso, E. Bodo, F. Gianturco, Computing a Three-Dimensional Electronic Energy Manifold for the LiH+ H 

  Li+ H₂ Chemical Reaction, J. Phys. Chem. A, 113 (2009), 1121-1128.
- [22] S. Bovino, M. Tacconi, F.A. Gianturco, D. Galli, F. Palla, On the relative abundance of LiH and LiH<sup>+</sup> molecules in the early universe: new results from quantum reactions, Astrophys. J, 731 (2011), 107.
- [23] S. Bovino, M. Wernli, F. Gianturco, Fast LiH destruction in reaction with H: quantum calculations and astrophysical consequences, Astrophys. J, 699 (2009), 383-387.
- [24] T. Roy, S. Mahapatra, Quantum dynamics of H+ LiH reaction and its isotopic variants, J. Chem. Phys, 136 (2012), 174313.
- [25] X. He, H. Wu, P. Zhang, Y. Zhang, Quantum State-to-State Dynamics of the  $H + LiH \rightarrow H_2 + Li$  Reaction, J. Phys. Chem. A, 119 (2015), 8912-8921.
- [26] X. He, P. Zhang, Z.X. Duan, Isotopic effect on the dynamics of the H/D + LiH/LiD reactions: Isotopic effect in the H + LiH system, Comput. Theor. Chem., 1084 (2016), 188-195.
- [27] F.V. Prudente, J.M. Marques, A.M. Maniero, Time-dependent wave packet calculation of the LiH+ H reactive scattering on a new potential energy surface, Chem. Phys. Lett., 474 (2009), 18-22.
- [28] Y. Liu, X. He, D. Shi, J. Sun, Theoretical study of the dynamics for the H+ LiH (v=0, j=0) to H<sub>2</sub>+Li reaction and its isotopic variants, Eur. Phys. J. D., 61 (2011), 349-353.
- [29] Y. Liu, X. He, D. Shi, J. Sun, Stereodynamics of the reaction H+ LiH (v=0, j=0)  $\rightarrow$  H<sub>2</sub>+ Li and its isotopic variants, Comput. Theor. Chem., 965 (2011), 107-113.
- [30] Z. Jiang, M. Wang, C. Yang, D. He, Influence of collision energy and reagent vibrational excitation on

- the stereodynamics of the reaction H+ LiH→ H<sub>2</sub>+ Li, Chem. Phys., 415 (2013), 8-13.
- [31] Z.-J. Jiang, M.-S. Wang, C.-L. Yang, D. He, The effects of collision energy and reagent vibrational excitation on the reactivity of the reaction H+ LiH: A quasiclassical trajectory study, Comput. Theor. Chem., 1006 (2013), 31-36.
- [32] G.Y. Sha, J.C. Yuan, C.G. Meng, M.D. Chen, Influence of early-staged energy barrier on stereodynamics of reaction of LiH( $\nu$ =0, j=0)+H $\rightarrow$ Li + H<sub>2</sub>, Chem. Res. Chin. Univ., 29 (2013), 956-961.
- [33] S. Gómezcarrasco, L. Gonzálezsánchez, N. Bulut, O. Roncero, L. Bañares, J.F. Castillo, State-to-state Quantum Wave Packet Dynamics of the LiH + H Reaction on Two Ab Initio Potential Energy Surfaces, Astrophys J., 784 (2014).
- [34] H. Zhai, W. Li, Y. Liu, Coriolis Coupling Influence on the H+ LiH Reaction, Bull. Korean Chem. Soc, 35 (2014), 151-157.
- [35] M.-K. Hsiao, K.-C. Lin, Y.-M. Hung, Quasiclassical trajectory calculations for Li ( $2^2P_1$ )+ H<sub>2</sub> LiH ( $X^1\Sigma^+$ )+ H: Influence by vibrational excitation and translational energy, J. Chem. Phys, 134 (2011), 034119.
- [36] J. Yuan, D. He, M. Chen, A new potential energy surface for the ground electronic state of the LiH<sub>2</sub> system, and dynamics studies on the H ( $^2$ S)+ LiH ( $X^1\Sigma^+$ )  $\rightarrow$  Li ( $^2$ S)+ H<sub>2</sub> ( $X^1\Sigma_g^+$ ) reaction, Phys. Chem. Phys., 17 (2015), 11732-11739.
- [37] J. Barnwell, J. Loeser, D. Herschbach, Angular correlations in chemical reactions. Statistical theory for four-vector correlations, J. Phys. Chem., 87 (1983), 2781-2786.
- [38] N.E. Shafer-Ray, A.J. Orr-Ewing, R.N. Zare, Beyond state-to-state differential cross sections: determination of product polarization in photoinitiated bimolecular reactions, J. Phys. Chem., 99 (1995), 7591-7603.
- [39] F. Aoiz, M. Brouard, P. Enriquez, Product rotational polarization in photon-initiated bimolecular reactions, J. Chem. Phys, 105 (1996), 4964-4982.
- [40] M.-L. Wang, K.-L. Han, G.-Z. He, Product rotational polarization in photo-initiated bimolecular reactions A+ BC: Dependence on the character of the potential energy surface for different mass combinations, J. Phys. Chem. A, 102 (1998), 10204-10210.
- [41] M.-L. Wang, K.-L. Han, G.-Z. He, Product rotational polarization in the photoinitiated bimolecular reaction A+ BC-> AB+ C on attractive, mixed and repulsive surfaces, J. Chem. Phys., 109 (1998), 5446-5454.
- [42] J. Liu, M. Wang, A. Gao, C. Yang, X. Sui, Z. Gao, Effects of the reagent rotational excitation on the stereodynamics of the reaction C(<sup>3</sup>P)+CH(X<sup>2</sup>Π)→C<sub>2</sub>+H, J. At. Mol. Sci., 6 (2015), 129-136.
- [43] D. Herschbach, Molecular dynamics of chemical reactions, Pure& Appl. Chem., 47 (1976), 61-73.

# **Appendix**

In this paper, the center of mass (CM) frame is shown in following figure.



k that denotes the reagent-approach directions is parallel to the z-axis, and y-axis is perpendicular to the x-z plane containing k and k' vectors. k' is the product-recoil directions. j' is the final product angular momentum and its polar and azimuthal angle is  $\theta_r$  and  $\phi_r$  respectively. The  $\theta_t$  between k and k' is defined as the scattering angle.

The distribution function  $P(\theta)$  describes the k - j' correlation and can be expanded in a series of Legendre polynomials as:

$$P(\theta_r) = \frac{1}{2} \sum [2k+1] a_0^{(k)} P_k(\cos \theta_r)$$
 (1)

The expanding coefficients  $a_0^{(k)}$  called polarization parameters are given by

$$a_0^{(k)} = \int_0^{\pi} P(\theta_r) P_k(\cos \theta_r) \sin \theta_r d\theta_r = \langle P_k(\cos \theta_r) \rangle$$
 (2)

The coefficients  $a_0^{(k)}$  are called orientation parameter (when k is odd) or alignment parameter (when k is even). As k = 2, the expression for the expansion coefficient  $a_0^{(2)}$  is written as,

$$a_0^{(2)} = \left\langle P_2(\cos\theta_r) \right\rangle = \left\langle P_2(j \cdot k) \right\rangle = \frac{1}{2} \left\langle 3\cos^2\theta_r - 1 \right\rangle \tag{3}$$

The dihedral angle distribution function  $P(\phi_r)$  representing the k - k' - j' vector correlation can be expanded in a series of Fourier as:

$$P(\phi_r) = \frac{1}{2\pi} \left( 1 + \sum_{even, n \ge 2} a_n \cos n\phi_r + \sum_{odd, n \ge 1} b_n \sin n\phi_r \right)$$
 (4)

with  $a_n = 2\langle \cos n\phi_r \rangle$  and  $b_n = 2\langle \sin n\phi_r \rangle$ .

The joint probability density functions of angles  $\theta_r$  and  $\phi_r$ , which describe the direction of j', can be written as  $P(\theta_r, \phi_r)$ .

$$P(\theta_r, \phi_r) = \frac{1}{4\pi} \sum_{kq} (2k+1) a_q^k C_{kq} (\theta_r, \phi_r)^*$$

$$= \frac{1}{4\pi} \sum_{k} \sum_{q>0} [a_{q\pm}^k \cos q \phi_r - a_{qm}^k \sin q \phi_r] C_{kq} (\theta_r, 0)$$
(5)

The expanding coefficients  $a_q^k$  can be estimated by:

$$\begin{aligned} a_{q\pm}^k &= 2 \Big\langle C_{k|q|}(\theta_r, 0) \cos q \phi_r \Big\rangle & (k \text{ is a even number}) \\ a_{qm}^k &= 2i \Big\langle C_{k|q|}(\theta_r, 0) \cos q \phi_r \Big\rangle & (k \text{ is a odd number}) \end{aligned}$$

The 3D angular distribution associated with the k - k'- j' correlation can be described by following expression in the CM frame:

$$P(\theta_t, \theta_r, \phi_r) = \sum_{kq} \frac{[k]}{4\pi} \frac{2\pi}{\sigma} \frac{d\sigma_{kq}}{d\omega_t} C_{kq} (\theta_r, \phi_r)^*$$
(6)

Where [k] = 2k + 1,  $C_{kq}(\theta_r, \phi_r)$  refers to the modified spherical harmonics. k denotes the quantum number of the product rotational angular momentum and q denotes the magnetic quantum number of the product rotational angular momentum. The real polarization dependent differential cross sections (PDDCSs) can be defined by:

$$\frac{2\pi}{\sigma} \frac{d\sigma_{kq\pm}}{d\omega} = \frac{1}{2} \sum_{\mathbf{k}_1 > q} (2k_1 + 1) s_{\{k\}q\pm}^{k_1} C_{\mathbf{k}_1 - \mathbf{q}}(\theta_r, 0)$$
 (7)

the coefficients  $s_{\{k\}q\pm}^{k_1}$  are given by

$$s_{\{k\}q+}^{k_1} = \sqrt{2} \left\langle C_{k_1 q}(\theta_t, 0) C_{k q}(\theta_r, 0) \cos(q \phi_r) \right\rangle$$

$$= \sqrt{2} \frac{1}{N_r} \sum_{i=1}^{N_r} C_{k_1 q}(\theta_t^{(i)}, 0) C_{k q}(\theta_r^{(i)}, 0) \cos(q \phi_r^{(i)})$$
(8)

$$s_{\{k\}q^-}^{k_1} = \sqrt{2} \left\langle C_{k_1 q}(\theta_t, 0) C_{k q}(\theta_r, 0) \sin(q \phi_r) \right\rangle \tag{9}$$

$$= \sqrt{2} \frac{1}{N_r} \sum_{i=1}^{N_r} C_{k_1 q}(\theta_t^{(i)}, 0) C_{k q}(\theta_r^{(i)}, 0) \sin(q \phi_r^{(i)})$$

$$s_{\{k\}0}^{k_1} = \left\langle P_{k_1}(\mathbf{c} \circ \mathbf{\theta}_t) P_k(\mathbf{c} \circ \mathbf{\theta}_r) \right\rangle$$

$$= \frac{1}{N_r} \sum_{i=1}^{N_r} P_{k_1}(\mathbf{c} \circ \mathbf{\theta}_t^{(i)}) P_k(\mathbf{c} \circ \mathbf{\theta}_r^{(i)})$$
(10)

where  $\theta_t^{(i)}$ ,  $\theta_r^{(i)}$  and  $\phi_r^{(i)}$  are the scattering angle and the polar angles of j' for the ith trajectory respectively, and  $N_r$  is the number of trajectories ending in a specific rotational state of the H<sub>2</sub> molecule. In particular, the DCS, corresponding to k =0, q =0, is calculated as

series in Legendre polynomials whose coefficients are the  $s_{\{k\}0}^{k_1}$  of the last equation.

Many photon-initiated bimolecular reaction experiments are sensitive to only those polarization moments with k=0 and k=2. So only the  $(2\pi/\sigma)(d\sigma_{00}/d\omega_t)$ ,  $(2\pi/\sigma)(d\sigma_{20}/d\omega_t)$ ,  $(2\pi/\sigma)(d\sigma_{21}/d\omega_t)$  are all calculated in this paper.